AJNR

3D Computerized Occlusion Rating of Embolized Experimental Aneurysms Using Noninvasive 1.5T MR Imaging

C. Sherif, S. Marbacher, J. Fandino, S. Erhardt, V. Neuschmelting, M. Killer, G. Mach and L. Remonda

AJNR Am J Neuroradiol 2012, 33 (4) 661-666
doi: https://doi.org/10.3174/ajnr.A2843
http://www.ajnr.org/content/33/4/661

ORIGINAL RESEARCH

3D Computerized Occlusion Rating of Embolized Experimental Aneurysms Using Noninvasive 1.5T MR Imaging

C. Sherif
S. Marbacher
J. Fandino
S. Erhardt
V. Neuschmelting
M. Killer
G. Mach
L. Remonda

BACKGROUND AND PURPOSE: For embolized cerebral aneurysms, the initial occlusion rate is the most powerful parameter to predict aneurysm rerupture and recanalization. However, the occlusion rate is only estimated subjectively in clinical routine. To minimize subjective bias, computer occlusion-rating (COR) was successfully validated for 2D images. To minimize the remaining inaccuracy of 2D-COR, COR was applied to 1.5T 3D MR imaging.

MATERIALS AND METHODS: Twelve experimental rabbit aneurysms were subjected to stent-assisted coil embolization followed by 2D DSA and 3D MR imaging. Subjective occlusion-rate (SOR) was estimated. Linear parameters (aneurysm length, neck width, parent vessel diameter) were measured on 2D DSA and 3D MR imaging. The occlusion rate was measured by contrast medium−based identification of the nonoccluded 2D area/3D volume in relation to the total aneurysm 2D area/3D volume. 2D and 3D parameters were statistically compared.

RESULTS: There were no limiting metallic artifacts by using 3D MR imaging. Linear parameters (millimeters) were nearly identical on 2D DSA and 3D MR imaging (aneurysm length: 7.5 ± 2.6 versus 7.4 ± 2.5, $P = .2334$; neck width: 3.8 ± 1.0 versus 3.7 ± 1.1, $P = .6377$; parent vessel diameter: 2.7 ± 0.6 versus 2.7 ± 0.5, $P = .8438$), proving the high accuracy of 3D MR imaging. COR measured on 3D MR imaging was considerably lower (61.8% ± 26.6%) compared with the following: 1) 2D-COR (65.6% ± 27.1%, $P = .0537$) and 2) 2D-SOR estimations (69.2% ± 27.4%, $P = .002$). These findings demonstrate unacceptable bias in the current clinical standard SOR estimations.

CONCLUSIONS: 3D-COR of embolized aneurysms is easily feasible. Its accuracy is superior to that of the clinical standard 2D-SOR. The difference between 3D-COR and 2D-COR approached statistical significance. 3D-COR may add objectivity to the ability to stratify the risk of rerupture in embolized cerebral aneurysms.

ABBREVIATIONS: CE = contrast-enhanced; COR = computerized occlusion rating; SOR = subjective occlusion rate; TOF = time-of-flight

For embolized ruptured and nonruptured cerebral aneurysms, the initial occlusion rate is the most powerful parameter to predict aneurysm rerupture and/or recanalization.[1-3] Despite its prognostic importance, the occlusion rate is only estimated subjectively in clinical routine. This introduces subjective bias. Additionally in most cases, these subjective estimations are performed on 2D images alone. It is difficult to evaluate complex 3D volumetric geometries with just 1 or 2 2D projection planes. As reported previously, this methodologic oversimplification of complex angioarchitecture is prone to subjective evaluation biases.[4-6]

To minimize this subjective estimation bias, COR was introduced for 2D images, and its validity was proved first on experimental and then on human cerebral aneurysms.[4,5,7] These methods have now been transferred to 3D imaging, to eliminate the remaining bias of indirect 2D evaluations.

Received April 2, 2011; accepted after revision July 11.

From the Departments of Neurosurgery (C.S., S.M., J.F., S.E.) and Neuroradiology (L.R.) Kantonsspital Aarau, Aarau, Switzerland; Cerebrovascular Research Group (C.S., S.M., J.F., S.E., V.N.), Department of Intensive Care Medicine, Berne University Hospital and University of Berne, Berne, Switzerland; Cerebrovascular Research Group (C.S., G.M.), Department of Biomedical Research, Medical University of Vienna, Vienna, Austria; Department of Neurology (M.K.), Paracelsus University, Salzburg, Austria; and Institute of Microelectronics (G.M.), Vienna University of Technology, Vienna, Austria.

Please address correspondence to Camillo Sherif, MD, Kantonsspital Aarau, Tellstr, CH-5000 Aarau, Switzerland; e-mail: camillo.sherif@meduniwien.ac.at

http://dx.doi.org/10.3174/ajnr.A2843

Ideally, 3D images should be obtained noninvasively to avoid unnecessary procedural complications of invasive DSA and to optimize cost-efficiency with a simple and precise outpatient examination. In fact, noninvasive 3D MR imaging is increasingly replacing invasive DSA in the clinical follow-up of embolized cerebral aneurysms.[8,9] Even for experimental rabbit aneurysms, the feasibility and excellent accuracy of noninvasive 3D MR imaging have been shown.[10-12]

The aim of the present study was to evaluate the feasibility of 3D-COR by using noninvasive 1.5T MR imaging in comparison with the present standard of 2D DSA in experimental endovascular aneurysms embolized by stent placement and/or coiling.

Materials and Methods

Aneurysm Creation

The protocol of this study was reviewed and approved by the local ethics committees. Venous-pouch arterial-bifurcation aneurysms were created in 12 adult female New Zealand white rabbits (2–3.6 kg). Surgical techniques and perioperative management are described elsewhere in detail.[13-15] To create an artificial bifurcation model, we microsurgically anastomosed the 2 common carotid arteries. Then a venous pouch, derived from the external jugular vein, was sutured as an aneurysm sac into this artificial bifurcation (Fig 1*A*). Complex bisaccular aneurysms (aneurysms No. 6, 7, 9) and broad-based aneurysms (aneurysm No. 8) were also created.[14]

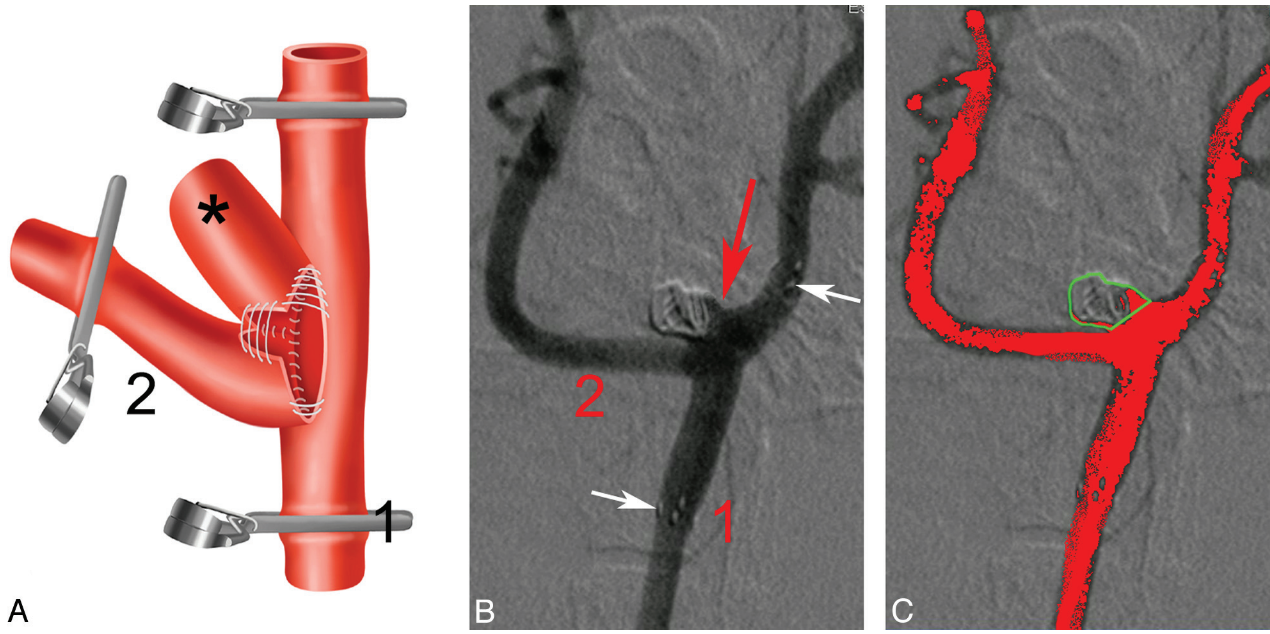

Fig 1. Microsurgical aneurysm creation and 2D DSA occlusion rating of aneurysm No. 3. *A*, Microsurgical creation of the venous-pouch arterial-bifurcation aneurysm in the rabbit. An artificial arterial bifurcation is created between the right (1) and left (2) common carotid artery. Then a venous pouch (*asterisk*) is sutured into the bifurcation, mimicking the aneurysm sac. *B*, 2D DSA anteroposterior view of the partially embolized aneurysm shows the unoccluded part of the aneurysm (*red arrow*). The small white arrows indicate the longitudinal radiopaque markers of the Neuroform stent. *C*, The borders of the contrast medium or coil-filled aneurysm parts and the orifice plane are outlined (green). The area filled or refilled by contrast medium within the total aneurysm area is defined on the posttreatment DSA, by using an attenuation-gradient-based distinction (red area within the aneurysm total area).

Aneurysm Embolization and 2D DSA

Four weeks after aneurysm creation, the animals underwent 2D DSA and embolization under general intravenous anesthesia. Images were obtained by rapid sequential 2D DSA at 2 frames per second by using a small focal spot at 66 kV and 125 mA (CAS 500; Toshiba Medical Systems, Tokyo, Japan). Intra-arterial bolus injection of nonionic iopamidol (0.6 mL/kg) as a contrast agent was administered at a rate of approximately 3 mL/s. For embolization and DSA, a 2.2F variable stiffness catheter (Tracker 10 or 18; Boston Scientific, Natick, Massachusetts) was placed in the common carotid artery via a standard transfemoral approach for selective DSA. The size of the aneurysm and the parent vessels was calibrated by paravertebrally placed skin clamps. Using fluoroscopy and road-mapping, we placed the microcatheter (Excelsior, Boston Scientific) and the microguidewire (Synchro, Boston Scientific) cranial to the aneurysm in the beginning of the intracranial portion of the internal carotid artery. After removal of the microcatheter, the stent (Neuroform 3, Boston Scientific) was introduced and detached over the aneurysm neck. For embolization purposes, the microguidewire was again introduced through the meshes of the stent into the aneurysm lumen. The catheter was positioned with the tip in the center of the aneurysm. Then coils (Guglielmi detachable coil 360°, Boston Scientific) were placed in the lumen of the aneurysm. We aimed at partial embolization of the aneurysm, by using 1–2 coils. The aneurysms No. 9–12 were embolized solely with HydroCoils (MicroVention Terumo, Aliso Viejo, California), again by using standard procedures. For final DSA, anteroposterior and lateral views were obtained together with a view of the working projection. We aimed to obtain aneurysms with a wide range of occlusion rates to evaluate the different occlusion-rating methods for all theoretic conditions.

Noninvasive 3D 1.5T MR Imaging

MRA was performed under general intramuscular anesthesia with ketamine and xylazine without mechanical ventilation by using a 1.5T scanner Magnetom Avanto Syngo B17 (Siemens, Erlangen, Germany). T2-weighted fast spin-echo (TR, 4300 ms; TE, 83 ms; FOV, 137–200 mm; 3-mm section thickness; matrix, 240 × 512) and 3D TOF MRA gradient-echo sequences were performed. After manual bolus injection of Gadovist (0.1-mL/kg gadubutrol, Schering, Berlin, Germany), CE 3D MRA was performed by using T1-weighted 3D fast-spoiled gradient-echo imaging (fast-spoiled gradient recalled; TR, 3.5 ms; TE, 1.3 ms; FOV, 137–200 mm; 1-mm section thickness; matrix, 352 × 512).

Subjective Occlusion Rating

Directly after each embolization procedure, the subjective occlusion rate of each aneurysm was estimated on DSA according to Roy et al.[3] For comparison with COR evaluations, total occlusion (Roy class 1) was then defined as a 100% occlusion rate, residual neck filling (Roy class 2) as a 95% occlusion-rate, and residual aneurysm fillings (Roy class 3) were estimated and rounded to 5% accuracy.

Computerized Evaluations and Occlusion Rating

2D DSA Evaluations. All quantitative measurements on the 2D DSA images were made by using custom software (CoilControl-2D; NVTec-Neurovascular Technologies, Ltd., Vienna, Austria). The observer was blinded to 2D-SOR and 3D-COR results. Two DSA projections were selected for evaluation. The selection criterion was to obtain a representative overview of the aneurysm occlusion, focusing on the recanalized neck together with the length axis of the aneurysms. Methods are described elsewhere in detail.[4,5] Briefly, the following parameters were measured on 2 calibrated representative 2D DSA images, as follows:

1) Neck width (millimeter): distance of the orifice plane, where the cranial borders of the parent arteries merged with the aneurysm outline.

2) Maximum length (millimeter): the longest distance between the orifice plane and the visible fundus of the aneurysm.

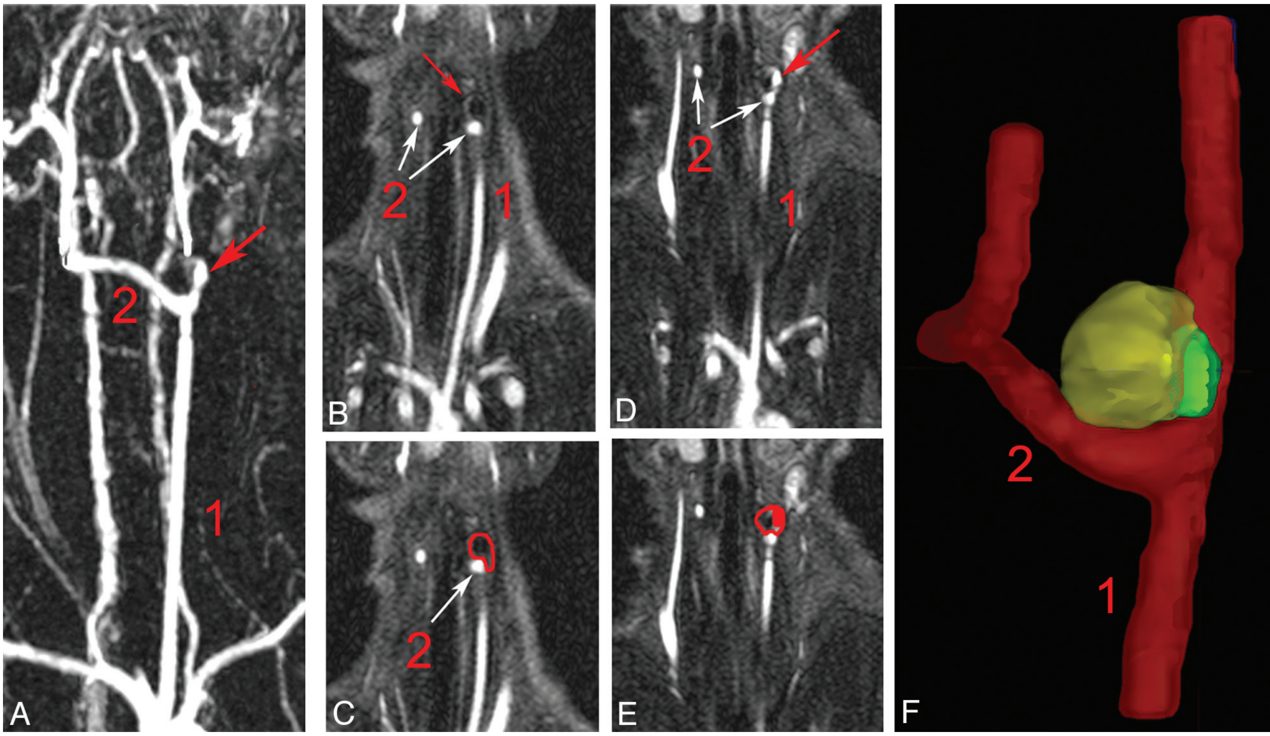

Fig 2. 3D MR imaging volumetric occlusion rating of aneurysm No. 3. *A*, Overview: right common carotid artery (1), left common carotid artery (2), and recanalized volume of the aneurysm (*red arrow*). *B*, The aneurysm outer border can be well-delineated (*red arrow*). *C*, The aneurysm outer border is circled in red. *B* and *C*, The embolized part of the aneurysm directly borders the left common carotid artery (*white arrow*, 2). *D*, The recanalized part (*red arrow*) of the aneurysm can be well identified. *E*, The recanalized aneurysm part is false-color-labeled (red area), and the aneurysm outer border is encircled (red). *F*, The 3D reconstruction: right common carotid artery, (1) left common carotid artery, (2) false-color-labeled embolized aneurysm volume (yellow), and false-color-labeled recanalized aneurysm volume (green).

3) Parent vessel diameter (millimeter): the diameter of the right common carotid artery just proximal to the stent.

4) Total aneurysm area (square millimeter): borders of the contrast medium or coil-filled aneurysm and the orifice plane outlined (Fig 1*B*, -*C*).

5) Recanalized area (square millimeter): the area filled or refilled by contrast medium within the total aneurysm area defined on the posttreatment DSA, by using an attenuation-gradient-based distinction (Fig 1*B*, -*C*).

Finally, the "occluded area" of the aneurysm was calculated as the difference of "total area" minus "nonoccluded area" and given as a 2D-COR as a percentage.

3D MR Imaging Evaluations. All quantitative measurements of the 3D MR images were made by using custom software (CoilControl-3D, NVTec-Neurovascular Technologies, Ltd.) (Fig 2). The observer was blinded to the results of 2D-COR and 2D-SOR. On each MR imaging section, the aneurysm borders were defined (Fig 2*B*, -*C*). Then the recanalized part of the aneurysm sac was depicted on every MR imaging section (Fig 2*D*, -*E*) and we measured the following parameters:

1) Aneurysm neck width, maximum length, and parent vessel diameter (see definitions above)

2) Total aneurysm volume (mm^3): To minimize coil and stent artifacts, we used low-field 1.5T MR imaging. On the source images of the CE MRA, it was possible to define the contours of the aneurysm sac (Fig 2*B*, -*C*). This definition of the aneurysm outer borders was performed on every MR imaging section of the aneurysm and the parent arteries. After automated 3D reconstruction (Fig 2*F*), the software calculated the respective volume.

3) Recanalized volume (mm^3): The volume within the aneurysm that was perfused by blood was measured (Fig 2*D*, -*E*). The definition of the blood perfused areas was performed on every MR section imaging the aneurysm or parent arteries. After automated 3D reconstruction (Fig 2*F*), the software calculated the recanalized volume. Finally, it was given as 3D-COR as a percentage of the total aneurysm volume.

Statistical Analysis

SAS 8.02 (SAS Institute, Cary, North Carolina) software was used for statistical analysis. The 2-tailed Wilcoxon matched-pairs signed rank test was used to compare the respective parameters of 3D MRA and 2D DSA evaluations. Data are presented as mean ± SD. A *P* value <.05 was considered significant.

Results

High imaging quality of all aneurysms could be obtained with 2D DSA and 3D MR imaging. There were no limiting coil or stent artifacts by using 1.5T CE-MRA. Aneurysm length and aneurysm neck could be measured in all created aneurysms. No technical problems during the performance of 2D DSA and 3D MR imaging were documented. The abdication of mechanical ventilation during 2D DSA and 3D MR imaging did not cause artifacts during the imaging. A comparison of 2D DSA and 3D MR imaging showed that the linear parameters (millimeter) were nearly identical: aneurysm length, 7.5 ± 2.6 versus 7.4 ± 2.5 (*P* = .2334); neck width, 3.8 ± 1.0 versus 3.7 ± 1.1 (*P* = .6377); and parent vessel diameter, 2.7 ± 0.6 versus 2.7 ± 0.5 (*P* = .8438) (Tables 1 and 2). The 3D computerized occlusion rate (61.8% ± 26.6%) showed considerable differences in comparison with 2D-COR (65.6% ± 27.1%, *P* = .0537) and subjective estimations (69.2% ±

Table 1: 2D DSA results of evaluations

	Length (mm)	Neck Width (mm)	Parent Vessel (mm)	2D-COR (%)	2D-SOR (%)
No. 1	4.30	3.10	1.90	100	100
No. 2	6.80	5.20	2.10	100	100
No. 3	5.90	2.90	1.90	89	85
No. 4	4.40	2.50	2.40	84	90
No. 5	6.10	3.30	2.10	83	95
No. 6	8.30	3.80	2.70	52	60
No. 7	11.70	4.80	3.40	30	30
No. 8	13.10	5.30	3.00	16	15
No. 9	8.20	4.80	2.80	46	50
No. 10	6.10	3.90	3.10	56	65
No. 11	8.20	3.40	3.80	45	50
No. 12	6.70	2.10	2.60	86	90
Mean	7.48	3.76	2.65	65.58	69.17
SD	2.55	1.02	0.58	27.06	27.37

Table 2: 3D MRA results of evaluations

	Length (mm)	Neck Width (mm)	Parent Vessel (mm)	Total Volume (mm^3)	Recanalization Volume (mm^3)	3D-COR (%)
No. 1	4.50	3.10	1.90	27.61	0.00	100.00
No. 2	6.70	5.10	2.10	111.26	3.34	97.00
No. 3	5.80	2.80	2.30	29.03	7.93	72.70
No. 4	4.50	2.40	2.30	16.55	4.09	75.30
No. 5	5.90	3.40	2.20	43.55	8.27	81.00
No. 6	8.10	3.30	2.70	73.86	42.69	42.20
No. 7	11.30	4.50	3.20	191.60	139.30	27.30
No. 8	13.40	5.10	3.10	291.84	261.20	10.50
No. 9	7.90	5.50	2.70	200.10	95.65	52.20
No. 10	6.20	4.20	3.00	68.68	32.97	52.00
No. 11	8.10	3.60	3.70	65.92	34.61	47.50
No. 12	6.50	1.90	2.60	14.74	2.33	84.20
Mean	7.41	3.74	2.65	94.56	52.70	61.83
SD	2.53	1.10	0.50	84.41	75.12	26.57

27.4%, $P = .002$), with the latter even reaching statistical significance. Most interesting, compared with 3D-COR, which was considered the most objective method, 2D-COR resulted in higher occlusion rates in 10 of 12 aneurysms (83.3%), and subjective 2D-SOR, in 11 of 12 aneurysms (91.7%).

Discussion

Recanalization of unruptured embolized cerebral aneurysms is a major problem in clinical practice. Between 10% and 20% of embolized aneurysms show recanalization during the long term, depending on their initial occlusion rates.[3] In addition, a low initial occlusion rate is the most powerful prognostic factor for aneurysm rerupture.[2] Despite this crucial clinical and prognostic importance, occlusion rate is only subjectively estimated in clinical routine. Reported rates of total aneurysmal occlusion (32%[16] to 76%[2]) and the incidence of aneurysmal neck remnants (17%[2] to 51%[16]) vary remarkably in the largest recently published series, underscoring the clinical relevance of the problem. To minimize subjective SOR estimation bias, COR was introduced for 2D DSA.[4,5] Its superiority over subjective occlusion-rate estimations, especially for the clinically most relevant aneurysms with high recanalization, was proved for experimental[4] and human aneurysms.[5] The next step was to transform these methods to 3D to overcome the remaining inaccuracy of 2D evaluations for 3D structures.

Recently, Yu et al[17] have also suggested using a compartmentalized 3D volumetric system for outcome analysis of coiled cerebral aneurysms. They applied complex image postprocessing, comprising a 2-step volume-extraction method, including a global thresholding method and an augmented vessel method that was used for volume calculation. The coiled aneurysm was compartmentalized into 3 volumetric components for quantitative analysis: 1) the aneurysm volume, 2) the volume of the coil mass, and 3) the volume of the uncoiled neck of the aneurysm. Changes in the volumetric data of these compartments at the time of follow-up provided a basis for a qualitative outcome analysis. The drawback of this method may be the need for special expensive postprocessing software and a time-consuming procedure. Additionally, their method is limited to DSA and is only applicable for aneurysms with follow-up 3D DSA available.

To guarantee wide clinical applicability, we chose the occlusion rate as the only available parameter with level 1 evidence,[2] instead of introducing a new complex volumetric grading system. We used noninvasive 3D MR imaging because we think it is mandatory to minimize interventional complications and to offer easily available and cheaper outpatient examinations.[9] In general, noninvasive MRA can deliver equivalent accuracy for cerebrovascular imaging, as shown by our group, for the evaluation of carotid artery stenosis.[18,19] Additionally MRA offers increased sensitivity to detect small amounts of blood flow compared with that of DSA. To detect contrast medium with DSA, a certain concentration of iodine must be present, and in some cases, this may easily be less than that observable by using x-ray angiography. MR imaging, on the other hand, has the potential to detect this level of flow.[20]

To guarantee wide clinical applicability, we chose 1.5T MR imaging, which represents a compromise between image resolution and the limitations of metallic artifacts. At 3T MR imaging, metallic artifacts may limit precise quantitative occlusion-rate evaluations or are impossible (no manufacturer approval) because of manufacturer proclaimed 3T MR imaging incompatibility of the respective embolization devices. Additionally, higher magnetic field strength could theoretically lead to inadequate inducted heating of the metallic implants and may result in consecutive inhibition of granulation tissue development and thus safe occlusion within the aneurysms.

In the present study, we used dynamic first 1.5T CE MRA protocols because these have been shown to offer the same accuracy as DSA.[20] However, Chung et al[21] have reported drawbacks of TOF MRA with maximum-intensity-projection reconstructions due to overestimations of the aneurysm height, as a consequence of overestimation of blood turbulence or due to loss of visualization of small or slow-flowing vessels. The authors suggested that CE MRA may represent a good solution to avoid size overestimation related to slow-flow patterns that occur especially in partially embolized aneurysms. Additionally, Gönner et al[22] and Deutschmann et al[23] described the varying sensitivity of 3D TOF MRA for the detection of aneurysm remnants, depending on their size, as a major limitation in human aneurysms. However, every MRA sequence could be used for 3D-COR.

Using noninvasive 1.5T CE MRA sequences and the custom-made software CoilControl, the present study showed easy feasibility of 3D computerized occlusion rating for coil and even stent-embolized aneurysms without limiting artifacts. Even though most aneurysms are coil-embolized only, the rationale for stent-assisted coiling in the present study was to evaluate possible stent artifacts, limiting universal applicability of 3D-COR.

For 2D DSA and 3D MRA, the evaluations resulted in nearly identical values for all linear parameters, proving the high accuracy of 3D MR imaging in comparison with DSA, which represents the present criterion standard for high-resolution imaging.

Comparison of Computerized Occlusion Rating Methods with Subjective Estimations

This feasibility study showed a clear superiority of 3D-COR over arbitrary subjective occlusion-rate estimations. Comparing COR of 3D MR imaging versus 2D DSA, we found considerable occlusion-rate differences. Even more, when 3D-COR was compared with subjective occlusion-rate estimations, these differences even reached statistical significance. In our opinion, these evaluations demonstrate an unacceptable bias of subjective occlusion rating as a standard clinical parameter. Moreover, subjective occlusion rating showed higher occlusion rates in 91.7% of all cases compared with 3D-COR. This can, theoretically, lead to dangerous follow-up decisions for single patients, with objective 3D-COR Roy class 3 aneurysms that are subjectively overestimated to Roy class 2 in clinical routine.

The differences between 3D-COR and 2D-COR nearly reached statistical significance ($P = .0537$). Such a clear trend was not expected by the authors. Maybe the difference could reach statistical significance in larger future series. To minimize 2D DSA bias, we selected meticulously representative 2D DSA projections for 2D-COR, trying to show the whole extent of the nonoccluded aneurysm neck as well the aneurysm dome. Despite this careful image selection, 2D-COR was higher in 83.3% of the aneurysms compared with 3D-COR. Greater differences were found in aneurysms with complex geometries (No. 6–9), showing the insufficiency of 2D-COR, especially for complex aneurysms. However, the small sample size did not allow subtype analysis. The trend to higher occlusion ratings of 2D-COR versus the "real" 3D-COR could theoretically lead to dangerous follow-up decisions, especially for patients with complex aneurysm geometries.

Concerning clinical applicability, 3D-COR can be performed easily and quickly by using the software CoilControl. It requires almost no additional clinical effort. In principle, 3D-COR can be performed with any 3D imaging technique and any 3D postprocessing image software. Such software is installed on nearly every modern imaging analysis workstation. Clinical application of 3D-COR could lead to more objective therapy decisions and better comparability of different series.

Limitations

Theoretic limitations are the different time points between 2D DSA and 3D MR imaging ($\leq$3 days). This time difference could lead to beginning thrombus organization and higher occlusion rates at 3D MR imaging. Theoretically different image-acquisition properties and imaging characteristics of the venous-pouch aneurysms could limit comparability of these experimental findings to human conditions, even though, especially for humans, dedicated and optimized sequences could further improve the imaging quality and, consequently, the postprocessing results.

The small sample size is a limitation for the representative power of this study. For ethical reasons, aiming at a proof of principle, we limited the animal experiments to 12 subjects.

Conclusions

For embolized experimental aneurysms, the present study proved easy feasibility and superiority of 3D-COR over subjective 2D-SOR estimations. Direct occlusion rating of the real 3D morphology showed unacceptable bias of 2D subjective occlusion-rate estimation, which is presently considered the clinical standard. The difference between 3D-COR and 2D-COR approached statistical significance with the highest differences in aneurysms with complex geometries. With proof of clinical applicability in larger human aneurysm series, 3D-COR could add objectivity to rupture risk stratification in aneurysms that either have been incompletely coiled or recur after treatment.

Disclosures: Camillo Sherif received scientific financial support from Boston Scientific Corporation, S&T Microsurgical Instruments, and Johnson & Johnson Inc. Dr. Sherif is a shareholder of NVTec-Neurovascular Technologies. Javier Fandino received funding from Johnson & Johnson Inc. Monika Killer—*UNRELATED*: *Grants/Grants Pending*: MicroVention, Terumo, *Payment for Lectures, Including Service on Speakers Bureaus*: MicroVention, Terumo, Comments: Aneurysm treatment at a regional neuroradiology conference in Augsburg, Germany, *Travel/Accommodations/Meeting Expenses Unrelated to Activities Listed*: Novomed, Comments: Travel expenses. The other authors have no conflicts of interest.

References

1. Molyneux A, Kerr R, Yu L-M, et al. **International Subarachnoid Aneurysm Trial (ISAT) of neurosurgical clipping versus endovascular coiling in 2143 patients with ruptured intracranial aneurysms: a randomised comparison of effects on survival, dependency, seizures, rebleeding, subgroups, and aneurysm occlusion.** *Lancet* 2005;366:809–17
2. Johnston S, Dowd C, Higashida R, et al. **Predictors of rehemorrhage after treatment of ruptured intracranial aneurysms: the Cerebral Aneurysm Rerupture After Treatment (CARAT) study.** *Stroke* 2008;39:120–25
3. Roy D, Milot G, Raymond J. **Endovascular treatment of unruptured aneurysms.** *Stroke* 2001;32:1998–2004
4. Sherif C, Plenk H Jr, Grossschmidt K, et al. **Computer-assisted quantification of occlusion and coil densities on angiographic and histological images of experimental aneurysms.** *Neurosurgery* 2006;58:559–66, discussion 559–66
5. Sherif C, Bavinzski G, Dorfer C, et al. **Computerized assessment of angiographic occlusion rate and coil density in embolized human cerebral aneurysms.** *AJNR Am J Neuroradiol* 2009;30:1046–53
6. Sherif C, Plenk H. **Quantitative angiographic and histopathologic evaluation of experimental aneurysms**. *AJNR Am J Neuroradiol* 2011;32:E33, author reply E34. Epub 2010 Dec 16
7. Cruise G, Shum J, Plenk H. **Hydrogel-coated and platinum coils for intracranial aneurysm embolization compared in three experimental models using computerized angiographic and histologic morphometry**. *J Mater Chem* 2007; 17:3965–73
8. Urbach H, Dorenbeck U, von Falkenhausen M, et al. **Three-dimensional time-of-flight MR angiography at 3 T compared to digital subtraction angiography in the follow-up of ruptured and coiled intracranial aneurysms: a prospective study.** *Neuroradiology* 2008;50:383–89
9. Schaafsma J, Koffijberg H, Buskens E, et al. **Cost-effectiveness of magnetic resonance angiography versus intra-arterial digital subtraction angiography to follow-up patients with coiled intracranial aneurysms.** *Stroke* 2010;41: 1736–42
10. Doerfler A, Becker W, Wanke I, et al. **Multimodal imaging in the elastase-induced aneurysm model in rabbits: a comparative study using serial DSA, MRA and CTA**. *Rofo* 2004;176:590–96

11. Krings T, Hans FJ, Moller-Hartmann W, et al. **Time-of-flight, phase contrast and contrast enhanced magnetic resonance angiography for pre-interventional determination of aneurysm size, configuration, and neck morphology in an aneurysm model in rabbits**. *Neurosci Lett* 2002;326:46–50
12. Sherif C, Marbacher S, Fandino J. **High-resolution three-dimensional 3 T magnetic resonance angiography for the evaluation of experimental aneurysms in the rabbit**. *Neurol Res* 2009;31:869–72
13. Sherif C, Marbacher S, Erhardt S, et al. **Improved microsurgical creation of venous-pouch arterial-bifurcation aneurysms in rabbits**. *AJNR Am J Neuroradiol* 2011;32:165–69
14. Marbacher S, Erhardt S, Ai Schläppi J, et al. **Complex bi-lobular, bi-saccular, and broad-necked microsurgical aneurysms formation in the rabbit bifurcation model for the study of upcoming endovascular techniques**. *AJNR Am J Neuroradiol* 2011;32:772–77
15. Sherif C, Fandino J, Erhardt S, et al. **Microsurgical venous pouch arterial-bifurcation aneurysms in the rabbit model: technical aspects**. *J Vis Exp* 2011; pii:2718
16. Jartti P, Isokangas J, Karttunen A, et al. **Early rebleeding after coiling of ruptured intracranial aneurysms**. *Acta Radiol* 2010;9:124–30
17. Yu S, So W, Chung A, et al. **A compartmentalized volumetric system for outcome analysis of coiled cerebral aneurysms: aneurysm-coil mass-neck outcome assessment system**. *Neurosurgery* 2009;64:149–55
18. Remonda L, Heid O, Schroth G. **Carotid artery stenosis, occlusion, and pseudo-occlusion: first-pass, gadolinium-enhanced, three-dimensional MR angiography—preliminary study**. *Radiology* 1998;209:95–102
19. Remonda L, Senn P, Barth A, et al. **Contrast-enhanced 3D MR angiography of the carotid artery: comparison with conventional digital subtraction angiography**. *AJNR Am J Neuroradiol* 2002;23:213–19
20. Agid R, Willinsky R, Lee S, et al. **Characterization of aneurysm remnants after endovascular treatment: contrast-enhanced MR angiography versus catheter digital subtraction angiography**. *AJNR Am J Neuroradiol* 2008;29:1570–74
21. Chung T, Joo J, Lee S. **Evaluation of cerebral aneurysms with high-resolution MR-angiography using a section-interpolation technique: correlation with digital subtraction angiography**. *AJNR Am J Neuroradiol* 1999;20:229–35
22. Gönner F, Heid O, Remonda L, et al. **MR angiography with ultrashort echo time in cerebral aneurysms treated with Guglielmi detachable coils**. *AJNR Am J Neuroradiol* 1998;19:1324–28
23. Deutschmann H, Augustin M, Simbrunner J, et al. **Diagnostic accuracy of 3D time-of-flight MR angiography compared with digital subtraction angiography for follow-up of coiled intracranial aneurysms: influence of aneurysm size.** *AJNR Am J Neuroradiol* 2007;28:628–34